

2014

Rapid-Scan EPR of Immobilized Nitroxides

Zhelin Yu
University of Denver

Richard W. Quine
University of Denver

George A. Rinard
University of Denver

Mark Tseitlin
University of Denver

Hanan Elajaili
University of Denver

See next page for additional authors

Follow this and additional works at: <https://digitalcommons.unl.edu/chemistryrajca>

 Part of the [Chemistry Commons](#)

Yu, Zhelin; Quine, Richard W.; Rinard, George A.; Tseitlin, Mark; Elajaili, Hanan; Kathirvelu, Velavan; Clouston, Laura J.; Boratyński, Przemysław J.; Rajca, Andrzej; Stein, Richard A.; Mchaourab, Hassane; Eaton, Sandra S.; and Eaton, Gareth R., "Rapid-Scan EPR of Immobilized Nitroxides" (2014). *Andrzej Rajca Publications*. 10.
<https://digitalcommons.unl.edu/chemistryrajca/10>

This Article is brought to you for free and open access by the Published Research - Department of Chemistry at DigitalCommons@University of Nebraska - Lincoln. It has been accepted for inclusion in Andrzej Rajca Publications by an authorized administrator of DigitalCommons@University of Nebraska - Lincoln.

Authors

Zhelin Yu, Richard W. Quine, George A. Rinard, Mark Tseitlin, Hanan Elajaili, Velavan Kathirvelu, Laura J. Clouston, Przemysław J. Boratyński, Andrzej Rajca, Richard A. Stein, Hassane Mchaourab, Sandra S. Eaton, and Gareth R. Eaton

Published in final edited form as:

J Magn Reson. 2014 October ; 247: 67–71. doi:10.1016/j.jmr.2014.08.008.

Copyright © 2014 Elsevier Inc.

Rapid-Scan EPR of Immobilized Nitroxides

Zhelin Yu^a, Richard W. Quine^b, George A. Rinard^b, Mark Tseitlin^a, Hanan Elajaili^a, Velavan Kathirvelu^{a,c}, Laura J. Clouston^d, Przemysław J. Boratyński^d, Andrzej Rajca^d, Richard Stein^e, Hassane Mchaourab^e, Sandra S. Eaton^a, and Gareth R. Eaton^a

^aDepartment of Chemistry and Biochemistry, University of Denver, Denver, Colorado, 80208 USA

^bSchool of Engineering and Computer Science, University of Denver, Denver, Colorado, 80208 USA

^cCurrent address – Department of Humanities and Sciences, National Institute of Technology Goa, Ponda, Goa 403 401, India

^dDepartment of Chemistry, University of Nebraska, Lincoln, NE 68588-0304 USA

^eDepartment of Molecular Physiology and Biophysics, Vanderbilt University Medical Center, Nashville, Tennessee 37232, USA

Abstract

X-band electron paramagnetic resonance spectra of immobilized nitroxides were obtained by rapid scan at 293 K. Scan widths were 155 G with 13.4 kHz scan frequency for ¹⁴N-perdeuterated tempone and for T4 lysozyme doubly spin labeled with an iodoacetamide spirocyclohexyl nitroxide and 100 G with 20.9 kHz scan frequency for ¹⁵N-perdeuterated tempone. These wide scans were made possible by modifications to our rapid-scan driver, scan coils made of Litz wire, and the placement of highly conducting aluminum plates on the poles of a Bruker 10" magnet to reduce resistive losses in the magnet pole faces. For the same data acquisition time, the signal-to-noise for the rapid-scan absorption spectra was about an order of magnitude higher than for continuous wave first-derivative spectra recorded with modulation amplitudes that do not broaden the lineshapes.

Keywords

immobilized nitroxide; Litz wire coils; rapid scan EPR; sucrose octaacetate glass; trehalose glass

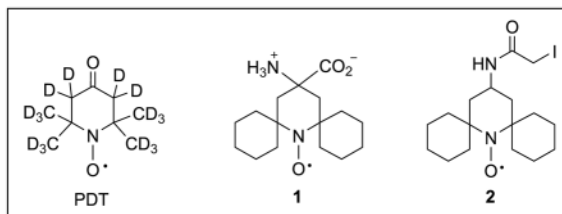
© 2014 Elsevier Inc. All rights reserved.

Corresponding author: Gareth R. Eaton, Department of Chemistry and Biochemistry, University of Denver, Denver, CO 80208, geaton@du.edu ph: 303-871-2980, fax: 303-871-2254.

Publisher's Disclaimer: This is a PDF file of an unedited manuscript that has been accepted for publication. As a service to our customers we are providing this early version of the manuscript. The manuscript will undergo copyediting, typesetting, and review of the resulting proof before it is published in its final citable form. Please note that during the production process errors may be discovered which could affect the content, and all legal disclaimers that apply to the journal pertain.

1. Introduction

In rapid-scan electron paramagnetic resonance (EPR) the magnetic field is scanned through resonance in a time that is short relative to the electron spin relaxation times [1]. The directly detected quadrature signal is obtained using a double-balanced mixer with the reference at the resonance frequency. By contrast conventional continuous wave (CW) EPR uses phase sensitive detection at the modulation frequency [1]. Deconvolution of the rapid-scan signal gives the absorption spectrum. Rapid-scan EPR has been shown to yield improved signal-to-noise (S/N) per unit time relative to continuous wave (CW) EPR for rapidly-tumbling nitroxides in fluid solution [2], spin-trapped superoxide [3], the E' center in irradiated fused quartz [4], amorphous hydrogenated silicon [5], N@C₆₀ diluted in C₆₀ [5], and the neutral single substitutional nitrogen centers (N_S⁰) in diamond [5]. With the exception of the piece-wise acquisition of the Hyde lab [6], the widest rapid-scan spectra reported so far were the 55 G scans of spin-trapped superoxide at X-band [3]. Among organic radicals, one very important case is immobilized nitroxide spin labels. In this paper we demonstrate that the technology developed in our laboratory for rapid scans can be extended to perform 155 G wide sinusoidal scans, which are wide enough to encompass the full spectrum of an immobilized nitroxide. Rapid scans were obtained for ¹⁴N-perdeuterated tempone (¹⁴N-PDT) and ¹⁵N-PDT in sucrose octaacetate and for T4 lysozyme spin labeled at positions 61 and 135 with iodoacetamide spiro cyclohexyl nitroxide **2** in a trehalose glass. The S/N for the rapid-scan spectra of the immobilized nitroxides is about an order of magnitude greater than for CW spectra of the same samples.



2. Methods

2.1 Sample preparation

Nitroxides ¹⁴N-PDT (perdeuterated 4-oxo-2,2,6,6-tetramethylpiperidinyloxy) and ¹⁵N-PDT (perdeuterated 4-oxo-2,2,6,6-tetramethylpiperidinyloxy-¹⁵N) were purchased from CDN isotopes (Quebec, Canada), and used as received. Solid ¹⁴N-PDT or ¹⁵N-PDT and sucrose octaacetate were mixed in ratios that would result in 0.50 mM or 0.050 mM solutions, respectively. The solids were ground gently in a mortar and pestle to mix the two components. The solid mixtures were placed in 4 mm outer diameter quartz EPR tubes, evacuated for 6 hr to remove oxygen, heated gently above the melting point, and cooled to form glasses [7]. Tubes were flame sealed. The concentrations of PDT in the samples were determined by comparison of the double integrated intensities with that for a standard sample of 0.56 mM tempone (4-oxo-2,2,6,6-tetramethylpiperidinyloxy) in toluene. The final concentrations of radical in the samples were 0.15 mM ¹⁴N-PDT and 0.018 mM ¹⁵N-PDT, and the numbers of spins in these samples were 2.3x10¹⁵ and 2.8x10¹⁴, respectively. These concentrations are lower than in the initial mixtures due to losses during the

evacuation and heating steps. Spirocyclohexyl amino acid nitroxide **1** was prepared at University of Nebraska as previously reported [8] and dissolved in 1:1 water:glycerol for relaxation time measurements. Iodoacetamide spirocyclohexyl spin label **2** was prepared at the University of Nebraska. For double electron-electron resonance (DEER) experiments [9] T4 lysozyme was spin-labeled at positions 61 and 135 by reaction of iodoacetamide spirocyclohexyl nitroxide **2** with cysteines introduced by site-directed mutagenesis. The preparation of the spin-labeled T4 lysozyme was performed at Vanderbilt University [9]. The solution of spin-labeled protein and a 10-fold excess of hen egg white lysozyme was mixed with 0.2 M trehalose in water, then spread on a watch glass and allowed to air dry in the dark for 48 hours before drying in vacuum for 6 hours. There were 1.4×10^{16} spins in the T4 lysozyme sample.

For electron spin relaxation time measurements MTSL (1-oxy-2,2,5,5-tetramethyl-3-pyrroline-3-methyl-methanethiosulfonate) was purchased from Toronto Research Chemicals, and tempone (4-oxo-2,2,6,6-tetramethylpiperidiny-*N*-oxy) was purchased from Sigma Aldrich.

2.2 EPR spectroscopy

CW and rapid-scan spectra were recorded on a Bruker E500T using a Bruker Flexline ER4118X-MD5 dielectric resonator, which excites spins over a sample height of about 1 cm [2,5]. Sample heights of about 4 mm were used to ensure uniform B_1 and scan field along the sample. The resonator Q is ~ 9000 for these nonlossy samples. The rapid-scan signals were recorded with a Bruker SpecJetII fast digitizer. The quadrature detection channels were calibrated with a small sample of the solid BDPA (1:1 α, γ -bisdiphenylene- β -phenylallyl:benzene) radical. Deconvolution and background removal procedures require that the phase difference between the two quadrature channels is close to 90° . Kronig-Kramers transformation of one channel and comparison with the other showed that the phase difference deviated from 90° by 7° . The phase difference between the two channels was corrected to 90° in the post-processing of the rapid-scan signals.

The sinusoidal scans were generated with the recently described scan driver [10]. The scan coils were constructed from 200 turns of Litz wire (255 strands of AWG44 wire). The coils have about 7.6 cm average diameter and were placed about 4 cm apart. The coil constant was 37.7 G/A, which is sufficient to generate scans up to 155 G wide with scan frequencies up to 13.4 kHz [10]. Mounting the coils on the magnet, rather than on the resonator, reduces the oscillatory background signal induced by the rapid scans. The placement of highly conducting aluminum plates on the poles of the Bruker 10" magnet reduces resistive losses in the magnet pole faces that arise from induced currents. The dielectric resonator decreases eddy currents induced by the rapidly-changing magnetic fields relative to resonators with larger amounts of metal. Data were acquired in blocks of 2 to 3 sinusoidal cycles. Scans are labeled with the rate in the center of the scan, which is $\pi f_s B_m \text{ G s}^{-1}$ where f_s is the scan frequency and B_m is the scan width.

To select the incident microwave powers for the CW and rapid scan experiments, power saturation curves were examined (Fig. 1). The amplitudes of CW spectra and rapid scan signals were measured as a function of microwave power. The incident powers were

converted to B_1 using the known resonator efficiency of about $3.8 \text{ G}/\sqrt{W}$ at Q of 9000 [5]. For signal-to-noise calculations rapid scan signals were deconvolved into EPR absorption spectra and processed as described in [11,12]. Figures 2 - 4 compare CW and rapid scan spectra measured at powers optimized for each measurement. The power selection was done using the following criterion. A linear least-squares fit through the point 0,0 and the signal amplitudes at the lowest 5 or 6 microwave powers was extrapolated to higher B_1 . The B_1 selected for data acquisition was the point at which the experimental signal amplitude was about 5% lower than the amplitude predicted by linear extrapolation of the non-saturated signal amplitude. The modulation frequency for the CW spectra was 100 kHz. The modulation amplitudes: ^{14}N -PDT in sucrose octaacetate (0.63 G), ^{15}N -PDT in sucrose octaacetate (0.9 G), ^{14}N -spin label on T4 lysozyme (1.8 G), were about 20% of B_{pp} . These combinations of parameters result in less than 2% line broadening relative to spectra obtained at lower modulation amplitude and smaller B_1 . The scan modulation frequencies for the rapid scan signals were limited by the constraints of the coil driver. At these scan frequencies the signal bandwidths were less than the resonator bandwidth [1] so resonator bandwidth did not contribute to spectral broadening.

The data acquisition times were about 10 s. The estimates of 10 s acquisition times were based on the following calculations, which are consistent with the relatively small overhead in the software. For CW spectra the acquisition time is the conversion time per point multiplied by the number of field steps. For rapid scans the acquisition time is $(1/f_s)$ multiplied by the product of number of scan cycles combined in the deconvolution software and the number of scans averaged.

Ambient temperature relaxation time measurements were obtained on a locally-built pulsed Xband spectrometer [13], equipped with a Bruker ER4118X-MS5 split ring resonator. Variable temperature measurements of amino acid nitroxide **1** were performed on a Bruker E580 as described previously [7,14]. Spin-spin relaxation times (T_2) were measured by two-pulse electron spin echo decay. Spin-lattice relaxation times (T_1) at 295 K were measured by inversion recovery and therefore may be slightly shortened by spectral diffusion. The temperature dependence of T_1 was measured by saturation recovery (Fig. S1). Relaxation times were calculated by fitting exponentials to the data using a locally written program that implements the Multifit algorithm [15].

2.3 Signal processing

Nitroxide tumbling correlation times, τ_R , in the rapid tumbling regime were determined by simulation of the CW lineshapes using the NLSL software [16].

The rapid-scan signals were deconvolved and background corrected [11,12]. The resulting spectra are the sum of up-field and down-field scans for the absorption and dispersion signals. The experimental dispersion spectra were converted into absorption spectra for summation with the experimental absorption spectra [17]. A post-processing Gaussian filter was applied to both CW and rapid-scan spectra. The cut-off frequency for the low-pass filter was selected to cause no more than 2% broadening of the full width at half maximum of the absorption spectra or the B_{pp} linewidth for first-derivative spectra. The bandwidth of the

first derivative spectrum is larger than for the absorption spectrum of the same signal [18]. The first derivative spectrum was therefore calculated by numerical differentiation of the deconvolved rapid-scan spectrum before low-pass filtering, with subsequent application of low-pass filtering. S/N is peak-to-peak signal amplitude (for CW) or signal amplitude (for rapid scan) divided by rms noise in baseline regions of the spectrum.

3. Results and Discussion

Sucrose octaacetate and trehalose form glasses at ambient temperatures. The EPR lineshapes for ^{14}N PDT in sucrose octaacetate (Fig. 2), ^{15}N PDT in sucrose octaacetate (Fig. 3) and for T4 lysozyme spin labeled with **2** in trehalose (Fig. 4) are consistent with immobilized nitroxides with $\tau_R > 10^4$ ps [19]. The spectra shown in Fig. 2 – 4 were obtained with ~ 10 s acquisition time, except for the CW spectrum of ^{15}N -PDT in sucrose acetate which was obtained with 5 min acquisition because of the low S/N .

3.1 Electron spin relaxation times

The X-band electron spin relaxation times at about 295 K for ^{14}N PDT in sucrose octaacetate, ^{15}N PDT in sucrose octaacetate, and T4 lysozyme spin labeled with **2** in trehalose are compared with values for more rapidly tumbling radicals in Table 1. T_1 in the vicinity of 10 μs for the immobilized nitroxides at 295 K is consistent with values reported previously for very slowly tumbling nitroxides [20,21]. Nitroxide T_1 increases as the tumbling correlation time, τ_R , becomes longer due to decreases in the contributions from spin rotation and from modulation of the anisotropic nitrogen hyperfine interaction [20,22,23]. The temperature dependence of T_1 for spirocyclohexyl nitroxides [24], including **1** (Fig. S1), is similar to that for methyl-containing nitroxides including tempone and MTSL [7,14]. For the strongly immobilized nitroxides at 295 K the dominant contributions to T_1 are the Raman process and a local mode, both of which depend on the properties of the glass. The longer value of T_1 for spin-labeled T4 lysozyme in trehalose than for PDT in sucrose octaacetate is proposed to arise because sucrose octaacetate is a softer glass than hydrogen-bonded trehalose [7].

PDT in water or 44% glycerol (τ_R is 9 or 19 ps, respectively) is near the rapidly-tumbling limit where motional averaging of anisotropy is nearly complete and T_1 dominates T_2 . As tumbling slows incomplete averaging of anisotropy causes T_2 to become very short and difficult to measure by pulsed EPR [25]. As tumbling slows further and the spectra approach the rigid limit, values of T_2 become longer. Values of T_2 about 0.5 μs at 295 K for ^{14}N PDT and ^{15}N -PDT in sucrose octaacetate and for T4 lysozyme spin labeled with **2** in trehalose indicate extensive immobilization [19], consistent with the rigid lattice lineshapes. For methyl-containing spin labels the averaging of electron spin couplings to inequivalent protons by rotation of the methyl groups causes a decrease in T_2 at temperatures between about 100 and 200 K. This process is absent in spirocyclohexyl nitroxides [8].

3.2 Comparison of CW and rapid-scan spectra

The power saturation curves for ^{14}N -PDT (Fig. 1) in sucrose octaacetate are typical of the samples studied. The region in which signal amplitude increases linearly with B_1 extends to

higher B_1 for the rapid-scan experiments than for CW, which permits use of higher microwave power without saturating the signal. This phenomenon has been observed previously in rapid scans of the E' center in irradiated fused quartz [4], nitroxides in fluid solution [2], amorphous hydrogenated silicon [5], N@C₆₀ diluted in C₆₀ [5], and the neutral single substitutional nitrogen centers (N_S⁰) in diamond [5]. In a rapid scan experiment the spin system is on resonance for a time that is shorter than in conventional CW, so higher B_1 can be used without saturation. The use of higher power (Table 2) and resulting increase in signal amplitude is a significant contributor to the improved S/N for rapid-scan spectroscopy [1].

The S/N for the rapid-scan absorption spectra is 6 to 30 times that for the CW first derivative spectrum (Table 2), which is a substantial advantage for weak signals. The S/N for the first derivative calculated from the rapid scan absorption spectrum has lower S/N than the original absorption spectra. This is due in part to the higher bandwidth of first derivatives, which limits the filtering that can be performed without broadening the spectrum [18]. The improved S/N for rapid-scan relative to CW spectra comes from three factors: (i) differences in signal amplitudes due to excitation of a small portion of the spectrum in the CW experiment vs excitation of the entire spectrum in rapid scan, (ii) the ability to use higher B_1 without power saturating the signal (Fig. 1), and (iii) the differences in the noise spectral densities in CW and rapid-scan spectra [1]. The improvement in S/N for rapid scan relative to CW was not as large for the spin-labeled T4 lysozyme sample as for the PDT samples. For the T4 lysozyme the linewidth is large due to the high spin concentration which permitted use of a higher modulation amplitude and therefore detection of a larger fraction of the signal amplitude than in the CW spectra of the PDT samples, which decreased the relative advantage of rapid scan. In addition, the large linewidths for the T4 lysozyme sample corresponds to a smaller signal bandwidth than for the narrow linewidths of the PDT signals. A higher scan rate for the T4 lysozyme sample would have been consistent with the resonator bandwidth and could have provided further improvement in S/N , but was not possible with the current hardware.

The S/N improvement for slowly tumbling spin-labeled protein samples that is provided by rapid scan EPR (Fig. 4) will be highly advantageous for biophysical studies.

Supplementary Material

Refer to Web version on PubMed Central for supplementary material.

Acknowledgments

The support of this work by NIH EB000557 (GRE and SSE), K25 EB016040 (MT), U54 GM084757 (HSM and RAS), and NSF CHE-1012578 (AR) and CHE-1362454 (AR) is gratefully acknowledged. We thank Virginia Meyer (University of Denver) for immobilization of the spin-labeled T4 lysozyme in glassy trehalose and Dr. Ying Wang (University of Nebraska) for purification of spin label 2.

References

1. Eaton, SS.; Quine, RW.; Tseitlin, M.; Mitchell, DG.; Rinard, GA.; Eaton, GR. Rapid Scan Electron Paramagnetic Resonance. In: Misra, SK., editor. Handbook of High Frequency EPR. Wiley; 2014. p. 3-67.

2. Mitchell DG, Quine RW, Tseitlin M, Eaton SS, Eaton GR. X-band Rapid-Scan EPR of Nitroxyl Radicals. *J Magn Reson.* 2012; 214:221–226. [PubMed: 22169156]
3. Mitchell DG, Rosen GM, Tseitlin M, Symmes B, Eaton SS, Eaton GR. Use of Rapid-Scan EPR to Improve Detection Sensitivity for Spin-Trapped Radicals. *Biophys J.* 2013; 105:338–342. [PubMed: 23870255]
4. Mitchell DG, Quine RW, Tseitlin M, Meyer V, Eaton SS, Eaton GR. Comparison of Continuous Wave, Spin Echo, and Rapid Scan EPR of Irradiated Fused Quartz. *Radiat Meas.* 2011; 46:993–996. [PubMed: 22003310]
5. Mitchell DG, Tseitlin M, Quine RW, Meyer V, Newton ME, Schnegg A, George B, Eaton SS, Eaton GR. X-Band Rapid-scan EPR of Samples with Long Electron Relaxation Times: A Comparison of Continuous Wave, Pulse, and Rapid-scan EPR. *Mol Phys.* 2013; 111:2664–2673.
6. Hyde JS, Bennett B, Kittell AW, Kowalski JM, Sidabras JW. Moving difference (MDIFF) non-adiabatic rapid sweep (NARS) EPR of copper(II). *J Magn Reson.* 2013; 236:15–25. [PubMed: 24036469]
7. Sato H, Kathirvelu V, Fielding AJ, Bottle SE, Blinco JP, Micallef AS, Eaton SS, Eaton GR. Impact of molecular size on electron spin relaxation rates of nitroxyl radicals in glassy solvents between 100 and 300 K. *Mol Phys.* 2007; 105:2137–2151.
8. Rajca A, Kathirvelu V, Roy SK, Pink M, Rajca S, Sarkar S, Eaton SS, Eaton GR. A spirocyclohexyl nitroxide amino acid spin label for pulsed EPR spectroscopy distance measurements. *Chem Eur J.* 2010; 16:5778–5782. [PubMed: 20391558]
9. Meyer V, Clouston L, Boraty ski PJ, Rajca A, Stein R, Mchaourab H, Eaton SS, Eaton GR. 2014 to be published.
10. Quine RW, Mitchell DG, Eaton SS, Eaton GR. A Resonated Coil Driver for Rapid Scan EPR. *Conc Magn Reson, Magn Reson Engineer.* 2012; 41B:95–110.
11. Tseitlin M, Rinard GA, Quine RW, Eaton SS, Eaton GR. Deconvolution of Sinusoidal Rapid EPR Scans. *J Magn Reson.* 2011; 208:279–283. [PubMed: 21163677]
12. Tseitlin M, Mitchell DG, Eaton SS, Eaton GR. Corrections for sinusoidal background and non-orthogonality of signal channels in sinusoidal rapid magnetic field scans. *J Magn Reson.* 2012; 223:80–84. [PubMed: 22967891]
13. Quine RW, Eaton GR, Eaton SS. Pulsed EPR spectrometer. *Rev Sci Instrum.* 1987; 58:1709–23.
14. Sato H, Bottle SE, Blinco JP, Micallef AS, Eaton GR, Eaton SS. Electron spin-lattice relaxation of nitroxyl radicals in temperature ranges that span glassy solutions to lowviscosity liquids. *J Magn Reson.* 2008; 191:66–77. [PubMed: 18166493]
15. Provencher SW. An eigenfunction expansion method for the analysis of exponential decay curves. *J Chem Phys.* 1976; 64:2772–2777.
16. Budil DE, Lee S, Saxena S, Freed JH. Nonlinear least-squares analysis of slow-motion EPR spectra in one and two dimensions using a modified Levenberg-Marquardt algorithm. *J Magn Reson A.* 1996; 120:155–189.
17. Tseitlin M, Quine RW, Rinard GA, Eaton SS, Eaton GR. Combining Absorption and Dispersion Signals to Improve Signal-to-noise for Rapid Scan EPR Imaging. *J Magn Reson.* 2010; 203:305–310. [PubMed: 20181505]
18. Tseitlin M, Eaton SS, Eaton GR. Uncertainty analysis for absorption and first-derivative EPR spectra. *Conc Magn Reson.* 2012; 40A:295–305.
19. Freed, JH. Theory of slow tumbling ESR spectra of nitroxides. In: Berliner, L.J., editor. *Spin Labeling: Theory and Applications.* Academic Press; New York: 1976. p. 53-132.
20. Owenius R, Terry GE, Williams MJ, Eaton SS, Eaton GR. Frequency Dependence of Electron Spin Relaxation of Nitroxyl Radicals in Fluid Solution. *J Phys Chem B.* 2004; 108:9475–9481.
21. Robinson BH, Haas DA, Mailer C. Molecular dynamics in liquids: spin-lattice relaxation of nitroxide spin labels. *Science.* 1994; 263:490–493. [PubMed: 8290958]
22. Robinson BH, Mailer C, Reese AW. Linewidth analysis of spin labels in liquids. I Theory and data analysis. *J Magn Reson.* 1999; 138:199–209. [PubMed: 10341123]
23. Eaton SS, Eaton GR. Relaxation times of organic radicals and transition metal ions. *Biol Magn Reson.* 2000; 19:29–154.

24. Kathirvelu V, Smith C, Parks C, Mannan MA, Miura Y, Takeshita K, Eaton SS, Eaton GR. Relaxation Rates for Spirocyclohexyl Nitroxyl Radicals are Suitable for Interspin Distance Measurements at Temperatures up to about 125 K. *Chem Commun.* 2009:454–456.
25. Millhauser GL, Freed JH. Two-dimensional electron spin echo spectroscopy and slow motions. *J Chem Phys.* 1984; 81:37–48.
26. Biller JR, Elajaili H, Meyer V, Rosen GM, Eaton SS, Eaton GR. Electron Spin Lattice Relaxation Mechanisms of Rapidly-Tumbling Nitroxide Radicals. *J Magn Reson.* 2013; 236:47–56. [PubMed: 24056272]

Research Highlights

- 155 G wide nitroxide spectra were scanned 26,800 times per sec.
- Signal averaged room temperature spectra were acquired in 10 s.
- Nitroxides were immobilized in sucrose octaacetate or trehalose glasses.
- Signal-to-noise was higher for rapid scan than CW for the same acquisition time.

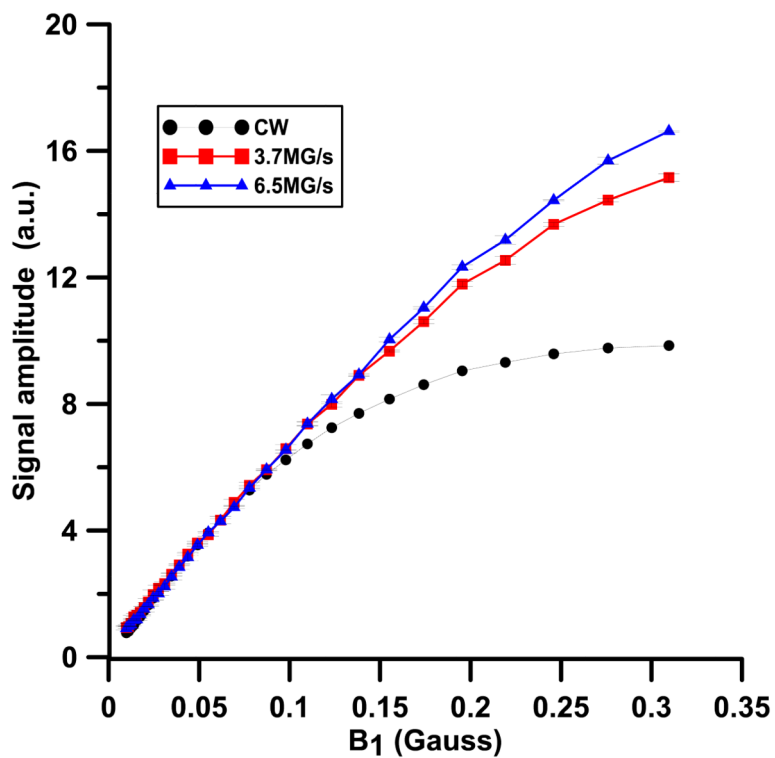


Figure 1. Power saturation curves at the peak of the absorption (rapid scan) or first derivative (CW) spectra of 0.15 mM ^{14}N -PDT in sucrose octaacetate at 293 K. The scan widths were 155 G and rapid-scan frequencies were 7.7 or 13.4 kHz. The amplitude of the CW spectra is scaled to match that obtained for the rapid scans at low B_1 .

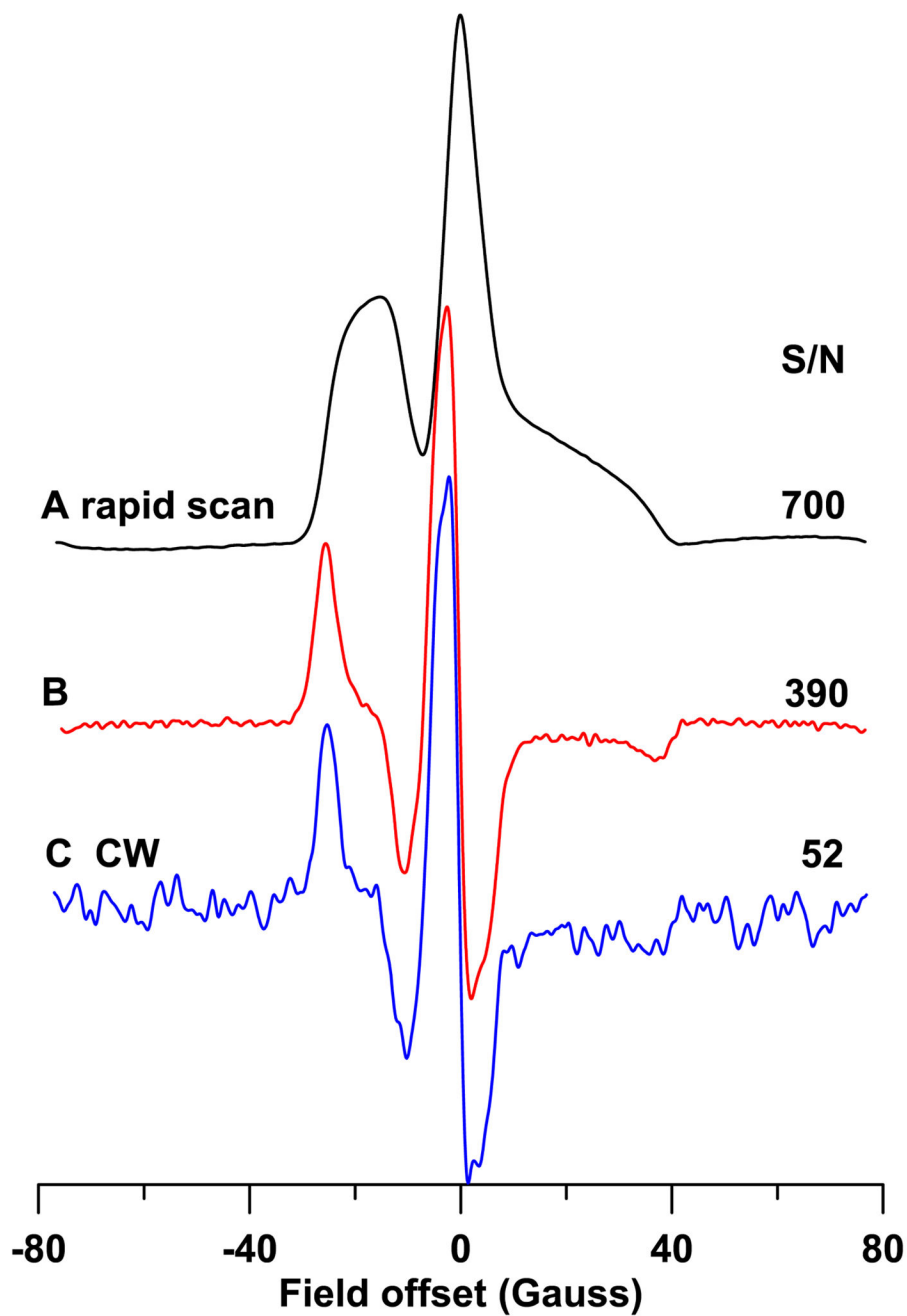


Figure 2. CW and rapid-scan spectra of 0.15 mM ^{14}N -PDT in sucrose octaacetate at 293 K obtained with 10 s acquisition time. (A) Absorption spectrum obtained by rapid scan with the parameters listed in Table 2, (B) first derivative spectrum obtained from (A) by numerical differentiation, and (C) field-modulated CW spectrum obtained with 100 kHz and 0.63 G modulation amplitude, which is 20% of $B_{\text{pp}} = 3.2$ G.

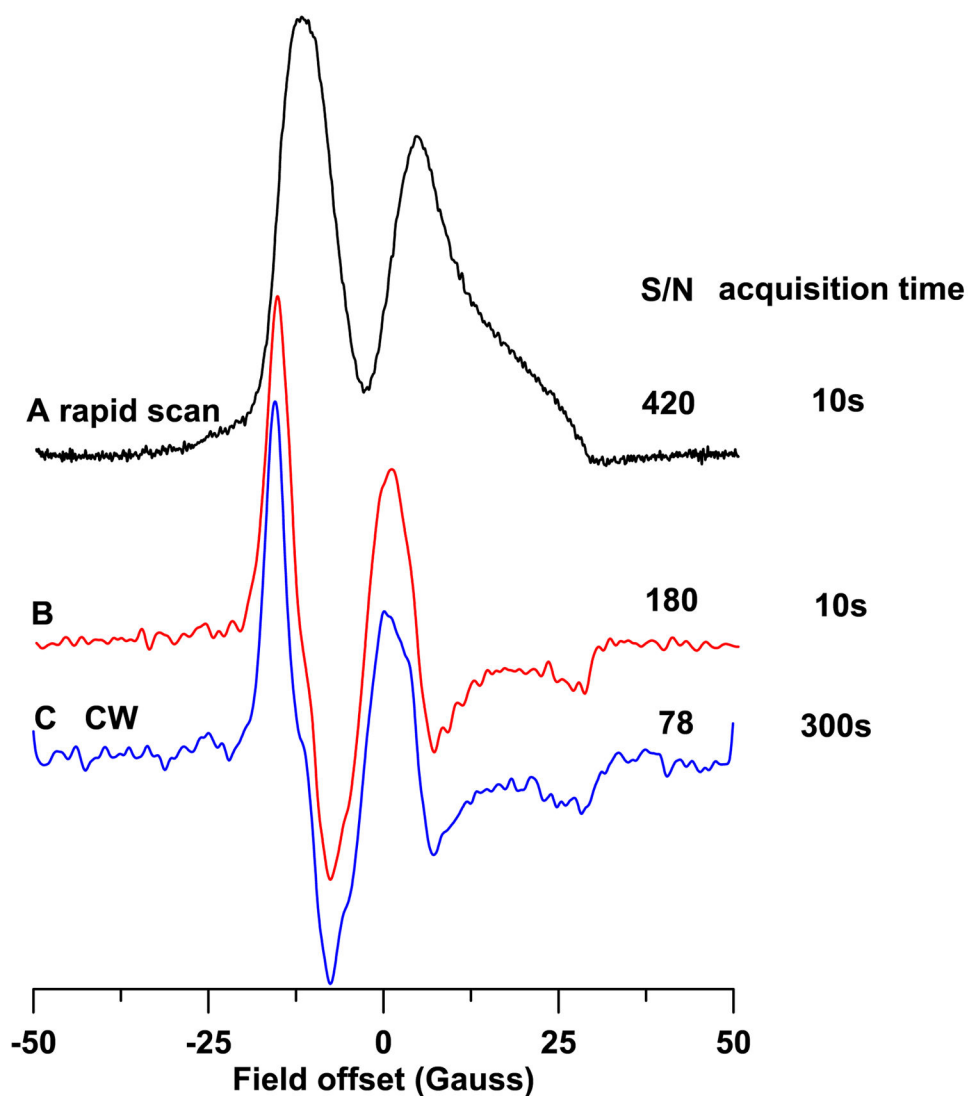


Figure 3. CW and rapid-scan spectra of 0.018 mM ^{15}N -PDT in sucrose octaacetate at 293 K. (A) Absorption spectrum obtained by rapid scan with the parameters listed in Table 2, (B) first derivative obtained from (A) by numerical differentiation, and (C) field-modulated CW spectrum obtained with 100 kHz modulation frequency and 0.9 G modulation amplitude, which is 20% of $B_{\text{pp}} = 7.23$ G. The data acquisition times were 10 s for (A) and 5 min for (C).

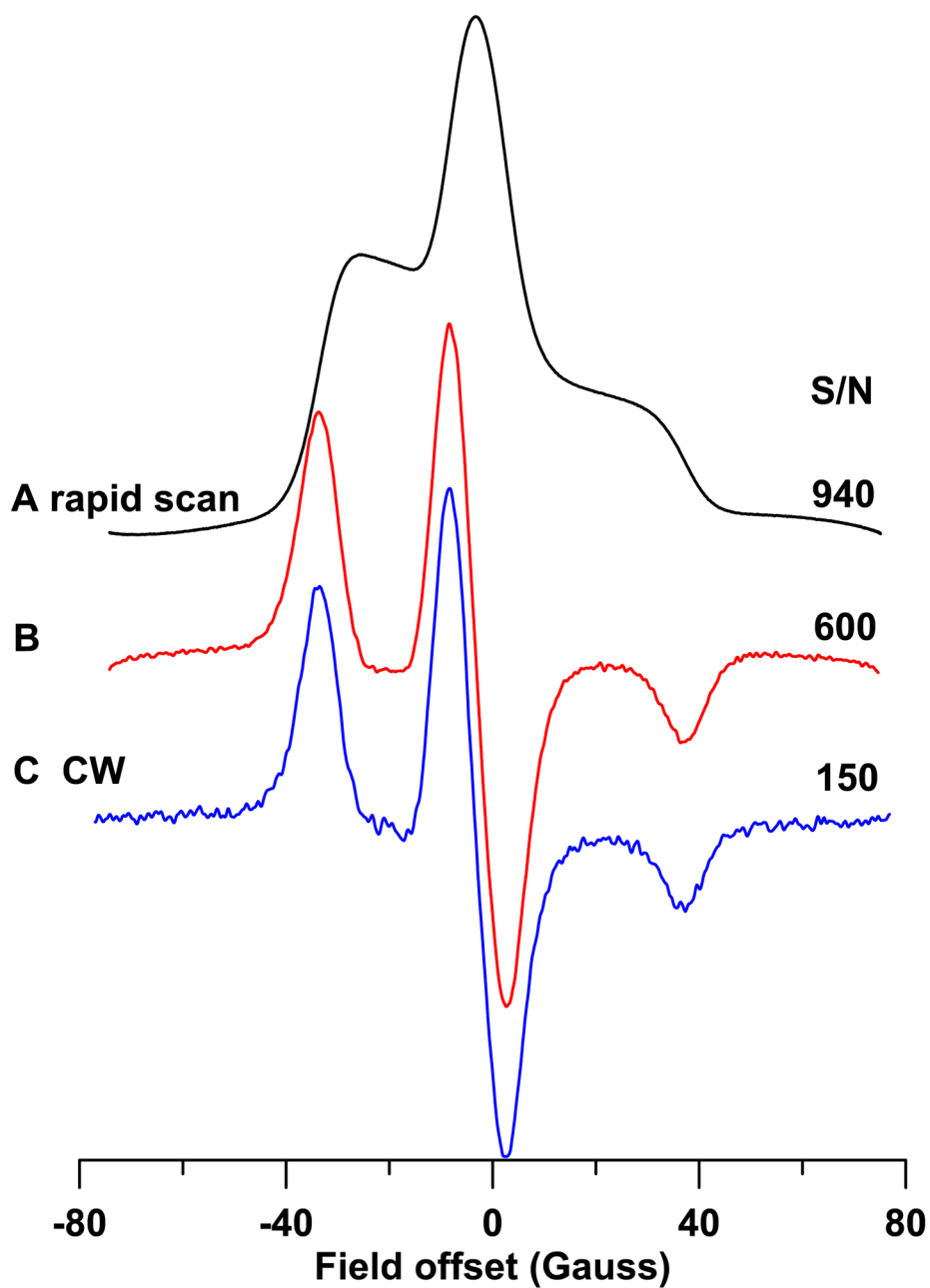


Figure 4. CW and rapid-scan spectra at 293 K of spin label **2** attached to T4 lysozyme obtained with 10 s acquisition times. (A) Absorption spectrum obtained by rapid-scan with the parameters listed in Table 2, (B) first derivative obtained from (A) by numerical differentiation, (C) field-modulated CW spectrum obtained with 100 kHz modulation frequency and 1.8 G modulation amplitude which is 20% of $B_{pp} = 1.06$ G

Table 1

X-band Electron Spin Relaxation Times at 293 to 295 K

Sample	Solvent	T ₁ (μs)	T ₂ (μs)	τ _R (ps)	reference
¹⁴ N-PDT	H ₂ O	0.57	0.48	9	[26]
¹⁴ N-PDT	44% glycerol	0.76	0.56	19	[26]
¹⁴ N-PDT	69% glycerol	2.2	0.25	50	[26]
MTSL	1:1 water:glycerol	2.2		130	This work
1	1:1 water:glycerol	4.0		350	This work
tempone	sucrose octaacetate	4.7			[7]
0.15 mM ¹⁴ N-PDT	sucrose octaacetate	6.0	0.77	> 10 ⁴	This work
0.018 mM ¹⁵ N-PDT	sucrose octaacetate	4.0	0.57	> 10 ⁴	This work
2 on T4 lysozyme	trehalose	1.4	0.52	> 10 ⁴	This work

Table 2

X-band CW and Rapid-scan EPR for ~10 s acquisition time

Sample	Scan frequency (kHz)	Sweep width (G)	Scan rate (MG/s)	B_1 for CW (mG)	B_1 for rapid scan (mG)	S/N of CW	S/N of rapid scan ^a	S/N ratio ^b
0.15 mM ¹⁴ N- PDT in sucrose octaacetate	13.4	155	6.5	24	49	52	700 (390)	13 (7.5)
0.018 mM ¹⁵ N- PDT in sucrose octaacetate	20.9	100	6.6	22	39	14 ^c	420 (180)	30 (13)
2 on T4 lysozyme	13.4	155	6.5	25	77	150	940 (600)	6 (4)

^aThe S/N for the absorption spectrum is shown, followed by the S/N for the first derivative in parentheses.

^bRatio of S/N for rapid scan absorption spectrum to that for CW, followed by ratio for first derivatives.

^cThe S/N for 5 min data acquisition time was 78. To correct to a 10 s acquisition time the S/N was divided by the square root of (300s/10s).